

The Effect of Cross-Beam Energy Transfer on Target Offset Asymmetry in Directly Driven Inertial Confinement Fusion Implosions

K. S. Anderson,¹ C. J. Forrest,¹ O. M. Mannion,¹ F. J. Marshall,¹ R. C. Shah,¹ D. T. Michel,^{1,2} J. A. Marozas,¹ P. B. Radha,¹ D. H. Edgell,¹ R. Epstein,¹ V. N. Goncharov,¹ J. P. Knauer,¹ and M. Gatu Johnson³

¹Laboratory for Laser Energetics, University of Rochester

²Applied and Theoretical Optics Department, ONERA, Palaiseau, France

³Plasma Science and Fusion Center, Massachusetts Institute of Technology

It is well known that at typical inertial confinement fusion (ICF) laser intensities, cross-beam energy transfer (CBET)¹ can cause significant laser energy losses to directly driven inertial confinement implosions. When CBET occurs, incoming laser light from one beam interacts with refracted, outgoing light from other beams, stealing some energy from the incoming light and scattering that energy away from the target along the path of the outgoing light rays. The result is a decrease in the ablation pressure, implosion velocity, and compression of the capsule, leading to lower fusion yield. One-dimensional simulations of direct-drive implosions at LLE have for years included CBET physics to better model implosions. However, because of the computational expense of including CBET physics in multidimensional simulations, these have often used a simpler, flux-limited Spitzer–Härm thermal transport method, where the flux limiter is variable in time and chosen to match the observables of more-detailed 1-D simulations, which include the nonlocal thermal transport (NLTT) and CBET physics. Because of this, few studies have been performed that include the effects of CBET on the symmetry of direct-drive ICF implosions.

One major source of laser nonuniformity is target mispositioning or offset. When the target is mispositioned with respect to the center of convergence of the laser beams, a perturbation with a dominant $\ell = 1$ mode is present in the illumination pattern on target, with the “hot side” (the side with higher illumination) being opposite the direction of the offset. Previous simulations without CBET have indicated that this $\ell = 1$ offset perturbation persists in time at high amplitude, resulting in highly degraded yields and distorted hot spots, even when target offsets are small, of the order of $10\ \mu\text{m}$ or about 2% of the radius of a typical capsule imploded on the 60-beam OMEGA Laser System. In contrast, fusion yields from cryogenic implosions on OMEGA show relatively low sensitivity to target offsets of this magnitude. This discrepancy between simulation and experiment has not been previously understood.

To study the effect of target offset in a more-controlled environment, experiments with room-temperature capsules were performed on OMEGA with prescribed offsets. These room-temperature experiments are simpler to field on OMEGA and require no cryogenic target handling or shroud, allowing more precise control of target positioning. Furthermore, these capsules have no cryogenic fuel layer, which typically represents a large and variable source of implosion nonuniformity and further complicates analysis. Results from these experiments were compared with 2-D *DRACO* simulations including the effects of CBET² plus a modified³ Schurtz–Nicolai–Busquet nonlocal thermal transport model (CBET–NLTT) as well as no-CBET *DRACO* simulations using a variable flux limiter (VFL). These comparisons illustrate the effect of CBET on the $\ell = 1$ laser drive uniformity, hot-spot x-ray core symmetry, and fusion yields. Note: the hydrodynamics and transport in *DRACO* are 2-D, but the laser ray-trace package is fully 3-D; this is sufficient to model target offset with CBET.

The normalized fusion yields from both the experiment and simulations are plotted in Fig. 1. The curves in Fig. 1 plot yields for *DRACO* simulations with varying offsets for a single shot (88575) with the CBET–NLTT model (solid red curve) and the VFL model (dashed blue curve). The simulations with the as-measured target offsets are shown with the red diamonds (CBET–NLTT)

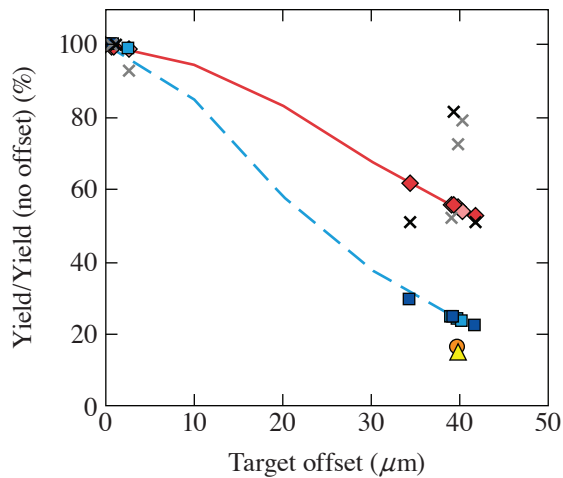


Figure 1

Normalized neutron yields for *DRACO* simulations (CBET–NLTT: red diamonds; VFL: blue squares) and experiment (x's). D₂ shots are shown in the lighter shades. Normalized yield trend lines are shown for shot 88575 varying the target offset in simulations (CBET–NLTT: solid red curve; VFL: dashed blue curve). For comparison, two simulations with a power-imbalance-induced $\ell = 1$ asymmetry equivalent to that of a 40- μm target offset at $t = 0$ were modeled (CBET–NLTT: orange circle; VFL: yellow triangle).

TC14804JR

and blue squares (VFL). Experimental data are shown with the x's. Normalized yields are shown for both the D₂ shots (lighter shades) and DT shots (darker shades). The simulation data show that the fusion yields are less sensitive to target offset when the CBET–NLTT model is used versus the VFL model, and that this difference occurs even for small target offsets. The variation in experimental yields in the offset shots is assumed to result from directional interactions with the target-mounting stalk and other systematic and/or random variations between shots, which are not modeled in the simulations.

For the D₂ shots, four x-ray framing cameras were deployed to collect time-resolved images of the coronal x-ray emission during the acceleration phase of the implosion from four different views. These images were then used to infer the centroid of the capsule as a function of time using the methodology of Ref. 4. Simulated time-resolved images were generated by post-processing *DRACO* data with *Spect3D*.⁵ The results from both experiment and simulation show that the center of the capsule experiences a linear spatial drift away from its initial position that is approximately linear when plotted versus the distance traveled by the shell. When the capsule radius had shrunk to $\approx 150 \mu\text{m}$, the distance traveled by the capsule center from the $t = 0$ position in the offset shots was measured experimentally to be between 9.2 to 10.0 μm along the offset direction with a 1.1- to 1.5- μm movement orthogonal to the offset direction (the measurement uncertainty was $\pm 1.0 \mu\text{m}$). The orthogonal movement is attributed to non-uniformity sources other than target offset. Reasonable agreement with experiment is seen in simulations with the CBET–NLTT model, which indicates the center drift along the offset direction is 12.0 μm . By contrast, the VFL model predicts 16.6- μm center drift, well outside the error bars.

On all shots, time-integrated x-ray images of the hot-spot core emission were obtained from the gated monochromatic x-ray imager (GMXI). The centroid of the core x-ray image was then calculated with respect to that of the target chamber center (TCC) reference shot for each series (D₂ and DT) to quantify the distance of the core in each offset shot relative to the reference target, following the methodology of Ref. 6. Time-integrated simulated images of the core x-ray emission were also generated from *DRACO* using *Spect3D* to compare with the GMXI images. The data are shown in Fig. 2. Figures 2(a) and 2(c) are the density contour of the target at peak compression and the time-integrated x-ray image from the VFL *DRACO* and *Spect3D* of shot 88581, respectively, whereas Figs. 2(b) and 2(d) are the same, respectively, for the CBET–NLTT model. Figure 2(e) is the experimental image. In each image, the position of TCC is shown with an x. The same analysis was done for the TCC reference shot 88578. Analysis shows that the distances between the centroid of x-ray emission of shots 88581 and 88578 are $61 \pm 2 \mu\text{m}$ for the experiment and 63 μm and 71 μm for the simulated CBET–NLTT and VFL, respectively. Only the CBET–NLTT result fits within the experimental error bars.

This mitigation of offset-induced nonuniformity by CBET effects can be understood geometrically. The shift of the target away from the center of beam convergence means that more laser light refracts past the target to interact with the incoming beams on the hot side, relative to those on the cold side. This stimulates more CBET losses on the hot side than on the cold side, effectively reducing the $\ell = 1$ illumination nonuniformity. This effect is also observed in simulations and experiments of polar-drive experi-

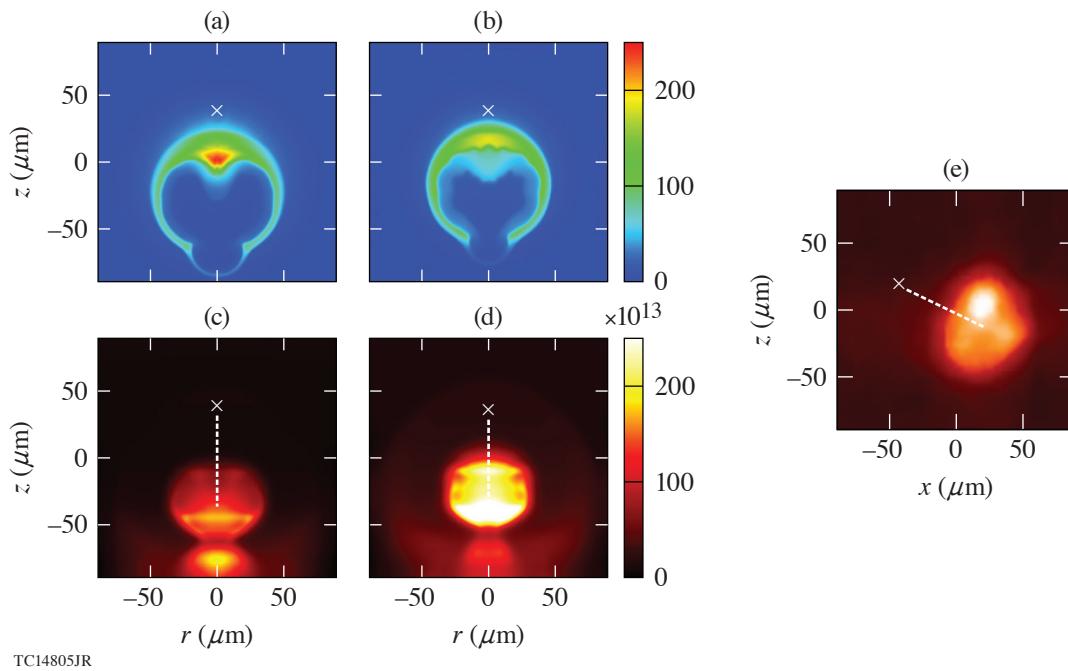


Figure 2

Density plot (g/cm^3) at stagnation from *DRACO* simulations of shot 88581 with (a) VFL and (b) CBET–NLTT. Simulated time-integrated x-ray images generated by *Spect3D* from these simulations are shown in (c) VFL and (d) CBET–NLTT. (e) The experimental image from GMX1c. In all images, the location of TCC is shown by the \times and the distance between TCC and centroid of emission indicated by the dashed white line.

ments² that show CBET is higher at the equator where beams are pointed away from the target center to improve illumination uniformity, and in experiments where the beam-to-target ratio is reduced⁷ to mitigate CBET. *DRACO*'s in-line scattered-light diagnostics support this conclusion, showing enhanced CBET-scattered light from the hot side of the target. To illustrate that this is a geometric effect arising from target offset, both CBET–NLTT and VFL *DRACO* simulations were performed, inducing an $\ell = 1$ using a prescribed laser power imbalance with the same initial mode amplitude as with the target offset of $40 \mu\text{m}$. The resulting normalized yields, shown in Fig. 1 by the orange circle (CBET–NLTT) and yellow triangle (VFL), are very close to each other and similar to the yield of the VFL offset simulation, indicating no mitigation of the power-imbalance–induced $\ell = 1$ by CBET.

In conclusion, CBET in direct-drive inertial confinement mitigates the implosion asymmetry caused by target offset. Simulations modeling target offset require a 3-D laser ray-trace model including CBET to accurately capture this asymmetry mitigation and to give better agreement with experimental observables.

This material is based upon work supported by the Department of Energy National Nuclear Security Administration under Award Number DE-NA0003856, the University of Rochester, and the New York State Energy Research and Development Authority.

1. I. V. Igumenshchev *et al.*, *Phys. Plasmas* **17**, 122708 (2010).
2. J. A. Marozas *et al.*, *Phys. Rev. Lett.* **120**, 085001 (2018).
3. D. Cao, G. Moses, and J. Delettrez, *Phys. Plasmas* **22**, 082308 (2015).
4. D. T. Michel *et al.*, *Phys. Rev. Lett.* **120**, 125001 (2018).
5. J. J. MacFarlane *et al.*, *High Energy Density Phys.* **3**, 181 (2007).
6. W. Grimble, F. J. Marshall, and E. Lambrides, *Phys. Plasmas* **25**, 072702 (2018).
7. D. H. Froula *et al.*, *Phys. Rev. Lett.* **108**, 125003 (2012).